IET Microwaves, Antennas & Propagation

Research Article

IET Journals
The Institution of Engineering and Technology

Frequency-selective substrate integrated waveguide front-end system for tracking applications

ISSN 1751-8725
Received on 24th January 2018
Revised 22nd March 2018
Accepted on 2nd April 2018
E-First on 24th April 2018
doi: 10.1049/iet-map.2018.0035
www.ietdl.org

Sara Salem Hesari[1], Jens Bornemann[1] ✉

[1]*Department of Electrical and Computer Engineering, University of Victoria, Victoria, BC, Canada*
✉ *E-mail: j.bornemann@ieee.org*

Abstract: A K-band frequency-selective front-end system for monopulse tracking applications is presented on a single layer of a substrate-integrated waveguide (SIW). The circuit comprises an antenna array of two Vivaldi antennas, a frequency-selective power combiner, and two frequency-selective SIW crossovers, which eliminate the need for subsequent filtering. Its performance is demonstrated in terms of sum and difference patterns, gain, and scattering parameters. In order to validate the design procedure, the monopulse tracking front end is fabricated and measured. It has a bandwidth of 540 MHz with an operating frequency range of 23.63–24.17 GHz. The sum and difference patterns are provided by in-phase and out-of-phase electric fields. The maximum achievable gain is 6.2 dB at the mid-band frequency, and a 30-degree field of view is obtained. The measurements are found to be in good agreement with simulations.

1 Introduction

Satellite communications and radar systems in the microwave and millimetre-wave ranges have attracted considerable attention for the development and design of monopulse tracking systems. Among the three main techniques, including sequential lobbing, conical scanning, and monopulse scanning, monopulse tracking is the most accurate and efficient technique [1].

Many researchers have worked on the design of monopulse tracking systems. The authors of [2] propose a radial line slot antenna with two simultaneous beams, one broadside beam and one conical beam for monopulse applications. A wideband monopulse tracking corrugated horn is presented in [3] which, by using two design techniques for a higher-order mode suppressor and a ring-loaded slot, provides good sum and difference radiation patterns. A time-division multiplexing monopulse antenna system is introduced in [4]. Although this circuit provides a 56-degree field of view and very good results in its operating bandwidth, the structure is complicated since it comprises a mode-former circuit which entails a four-way power splitter including Wilkinson power dividers, four switched-line phase shifters and the stacked circularly polarised antenna array which is composed of four edge-fed patches and four parasitic patches. A high gain 2×2 array using multiple horns and dielectric rods is designed in [5] for tracking applications, covering a field of view of about 14°. A waveguide slot array antenna, which includes 820 slots and four centre-fed sub arrays, is presented in [6]. This design not only has a narrow field of view but also suffers from a complicated fabrication process since the entire array is divided into four mechanical layers for manufacturing. A low profile patch antenna with a dual probe fed and a 180-degree directional coupler is combined to provide a monopulse tracking system in [7]. A crescent-shaped radiating element, which is fed from two sides at an angle close to 90° by two coaxial feeds, is used to design a monopulse antenna in [8].

With the advent of substrate integrated waveguide in the microwave and millimetre-wave technology and its advantages like low cost, high efficiency, low loss and planar structure, which allows easy integration with other components, many design engineers have started to use substrate-integrated waveguide (SIW) technology for designing monopulse antennas and tracking systems. For instance, a dual V-type linearly tapered slot antenna using a multimode SIW feeding technology is introduced in [9] which is able to produce the sum and difference patterns by using only a single element. A new Ka-band SIW slot array antenna is introduced in [10] which qualifies as a monopulse tracking system. In this design, the monopulse comparator, the sub arrays, and feeding system are integrated into a single, planar substrate layer. A monopulse antenna system is designed in [11] by combining a microstrip hybrid ring coupler, a power divider, and SIW slot array antennas. An SIW monopulse network is designed in [12] for a Ku-band tracking system. This design comprises four eight-way power dividers, four phase shifters, four 3 dB couplers and a patch array antenna on different substrates, which makes not only fabrication but also the design procedure complicated. Another monopulse tracking system is proposed in [13] including four 3-dB directional couplers, four 90-degree phase shifters, four 16-way dividers, and four 16×16 slot antenna sub-arrays.

In this paper, we propose a novel SIW front-end system for monopulse tracking applications which not only uses fewer components in comparison with other systems, but also is compact, easy to fabricate, provides good performance over its operating bandwidth and, most importantly, possesses inherent bandpass selectivity which makes filtering within the RF receiver chain obsolete. A monopulse amplitude comparison technique is usually preferred to other monopulse techniques since its implementation is much easier and also has a good performance [14]. Since both amplitude and phase are analysed for tracking signals and calculating the field of view, we use a combination of both techniques, thus amplitude and phase comparison is employed. By analysing the sum and difference radiation patterns, the angular field of view is determined. Substrate integrated waveguide technology is used for all components to obtain minimum loss and ease of fabrication. All components are designed and fabricated on a single layer of the substrate.

In Section 2, we introduce the design process which comprises the design of an end-fire Vivaldi antenna, a frequency-selective power combiner, and a frequency-selective SIW crossover structure with high isolation. In the end, the front-end system, which is a combination of all three components, is introduced. In Section 3, the performance of the system is presented and discussed which includes the measured and simulated sum and difference radiation patterns, gain and scattering parameters. Section 4 concludes the paper.

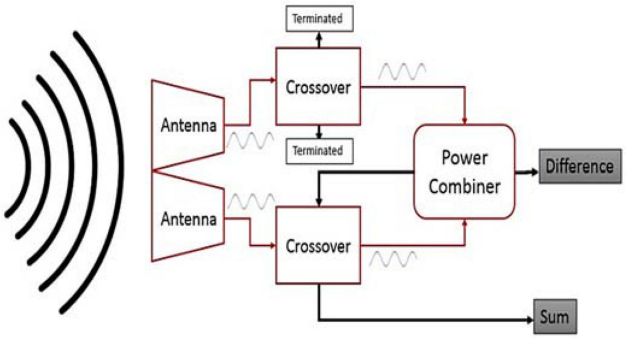

Fig. 1 *System block diagram for tracking applications*

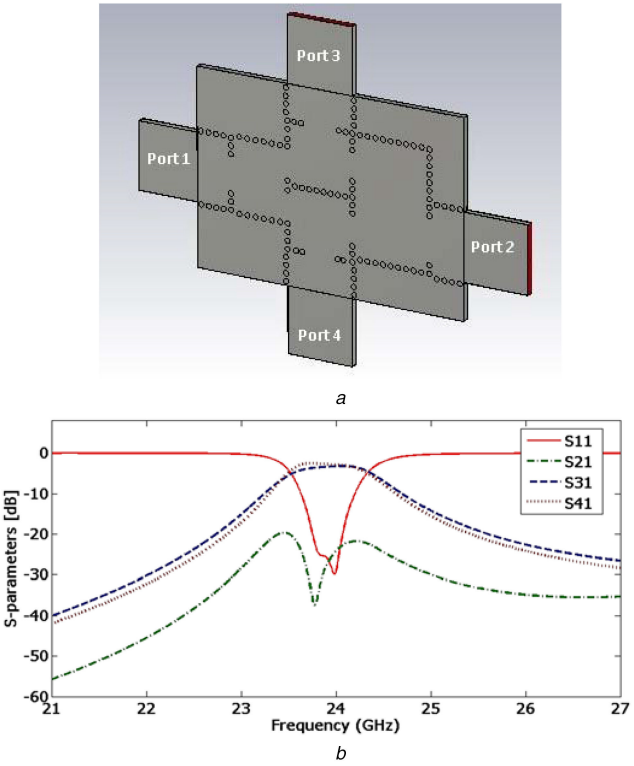

Fig. 2 *Frequency-selective SIW power divider/combiner*
(a) Prototype, ***(b)*** S-parameter analysis for port 1

2 Design procedure

A block diagram of the proposed system is presented in Fig. 1. It combines two SIW crossovers, a sum-difference power combiner and an antenna array of two Vivaldi antennas. Owing to its planar structure, the entire system can be fabricated in single-layer SIW technology. All individual components are designed and optimised on the same substrate to work over the specified pass band of the system.

The two Vivaldi antennas receive the signals and send them to the filtering SIW crossovers that are located perfectly symmetric to provide the same amplitude and phase at their outputs. The SIW crossover is designed with an isolation better than 24 dB, which prevents interference between the signals from the crossed paths. The top crossover in Fig. 1 is used as a transition to keep the structure symmetric. Only two ports are actually used, and the cross ports are terminated by matched waveguide ports in the full-wave simulator and by the absorber material during measurements. The lower crossover plays the main role in this system. It receives the signal from the antenna and passes it towards the power combiner to port 4 (cf. Fig. 2*a*), and then the power combiner combines both received signals from ports 3 and 4 and sends the in-phase signal to the lower crossover to pass it towards the sum port. The SIW crossover's high isolation feature prevents the oncoming signals to interfere at the junction, i.e. no interference between signals from the power divider to the sum port and from the lower Vivaldi antenna to the power combiner.

2.1 Power combiner

Design specifications of power combiners vary according to the application, as it is the entire project description that defines the design requirements. The fastest method for SIW power divider/combiners is to first design an all-dielectric-filled rectangular waveguide component, then transfer it to SIW using the equivalent waveguide width [15] and finally optimise the combiner in order to obtain the desired performance.

Since this paper focuses on a system with frequency selectivity, a second-order bandpass filtering power combiner with two input and two output (sum and difference) ports is selected. As shown in Fig. 2*a*, the proposed combiner utilises inputs ports 3 and 4, providing the sum (in phase) at port 1 and the difference (out of phase) at port 2. The principle design guidelines of this specific SIW component are detailed in [16, 17]. Fig. 2*b* shows the performance of the power combiner after optimisation in CST Microwave Studio 2017. The second-order bandpass characteristic is clearly visible, and the isolation between the two output ports 1 and 2 is better than 20 dB.

Note that owing to the type of resonators used, this component is comparable in functionality to a rat-race ring or a Magic Tee, just with the added advantage of a second-order bandpass filtering function in all transfer paths [17]. Port 1 receives the in-phase signals after they pass the two-resonator filter, and port 2 obtains the difference of the signals due to a 180-degree path difference created by the TE_{102}-mode resonator attached to port 2 [16].

2.2 Vivaldi antenna

A tapered slot antenna is an ideal candidate for a tracking front end since it has a wide bandwidth, high gain, directive radiation pattern and a planar structure that integrates easily with other planar circuitry. In the aperture, the electric field of the Vivaldi antenna is parallel to the substrate while that in SIW structures is perpendicular to the substrate. The tapered blade structure causes the rotation of the electric field from horizontal to vertical direction until the distance between the two blades is far enough to permit radiation. For improving cross polarisation, reducing the VSWR and increasing on-axis gain, comb-like corrugation is applied [18]. The antenna is initially designed based on the one used in [19], but some fine optimisation is applied based on the current system's requirements. The antenna prototype, return loss and radiation pattern are shown in Fig. 3. The proposed Vivaldi is optimised for a high gain which is about 9.58 dB over the bandwidth. It also has a return loss better than 15 dB from 19.2 to 28.6 GHz.

2.3 SIW crossover

An easy-to-fabricate and frequency-selective 0-dB SIW crossover structure is presented in [20] and is used as the main model for this paper. This cruciform design includes two resonators; the centre resonator is formed by two cascaded vias at the centre of the transition and utilises a TE_{102}-mode resonance. The second and third resonators in each path are applied for increasing the bandwidth; they are half-wavelength TE_{101}-mode resonators. As is indicated in Fig. 4*a*, both resonators have their zero at the centre of the crossover which improves the isolation level when two perpendicular ports are excited at the same time. As will be shown in the following section, the SIW crossover is required to demonstrate high isolation in order to isolate the output port of the power combiner from the input of one of the antennas. Fig. 4*b* presents the simulation results, demonstrating return loss better than 25 dB and isolation better than 24 dB from 23.4 to 24.2 GHz.

2.4 Front-end system

All individual components are designed and separately fine-optimised (by the Powell method) in the full-wave electromagnetic simulator CST STUDIO SUITE 2017 before integrating them on a single layer of the substrate. Microstrip-to-SIW transitions based

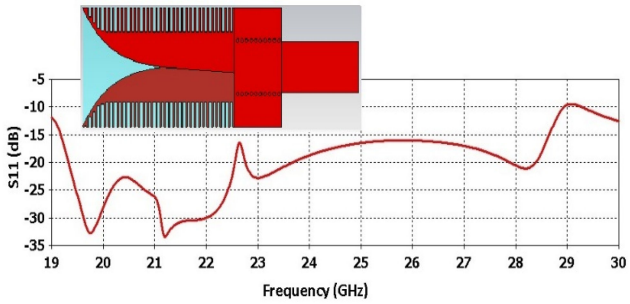

a

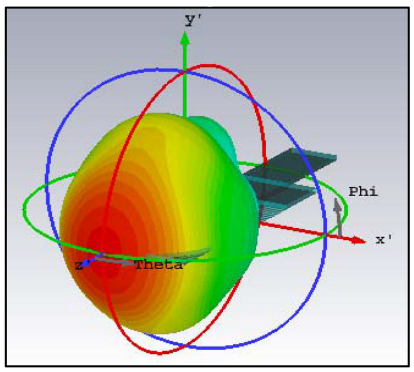

b

Fig. 3 *Vivaldi antenna*
(a) Return loss, ***(b)*** Radiation pattern at 24 GHz with 9.58 dB gain

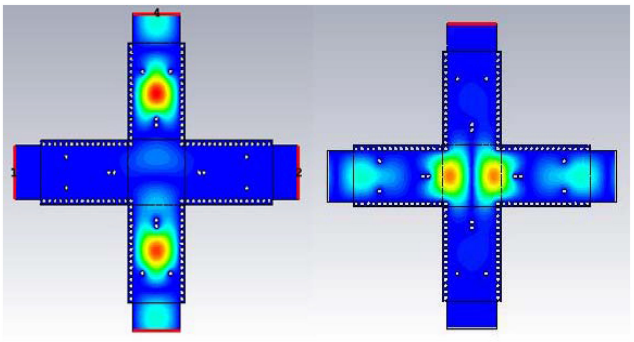

a

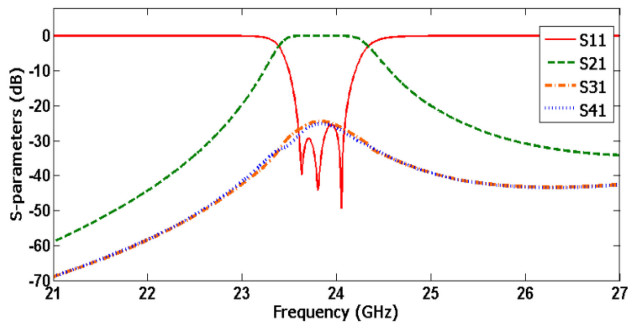

b

Fig. 4 *High-isolation frequency-selective SIW crossover*
(a) Electric fields, ***(b)*** S-parameters

on [21] are applied for connecting the sum and difference ports to K-connectors.

The basic block of the power combiner consists of the planar four-cavity structure with three of them operating in SIW TE_{101} modes and one in the SIW TE_{102} mode, and each cavity is coupled to one port of the unit [17]. The power combiner receives signals at ports 3 and 4, and the in-phase signal comes out through port 1, passes the crossover and arrives at the sum port. The signal with 180-degree phase difference goes through port 4 and is received at the difference port. Fig. 5 demonstrates the electric field over the

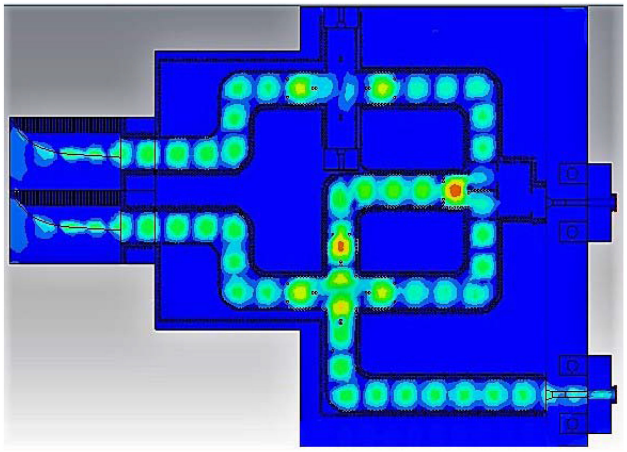

Fig. 5 *Electric field pass while a plane wave source is placed exactly in front of the frequency-selective tracking front end*

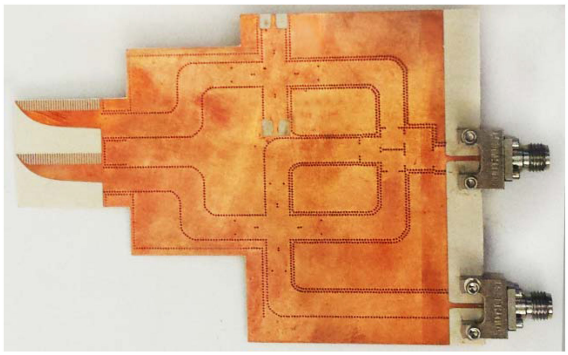

a

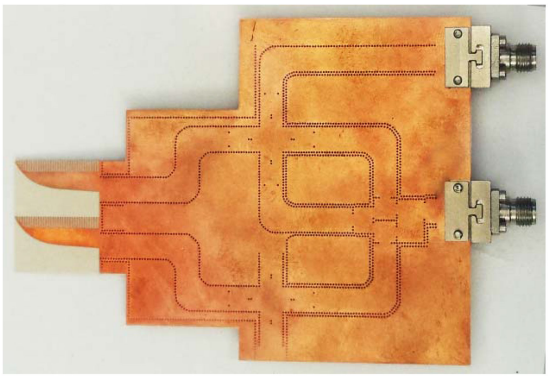

b

Fig. 6 *Fabricated frequency-selective front-end system for tracking applications*
(a) Top view, ***(b)***Bottom view

entire structure while the transmitter is exactly in front of the system ($\theta = 0°$).

3 Experimental results

The front-end system with bandpass characteristic for tracking applications is designed and fabricated on Rogers 6002 substrate with relative permittivity of $\varepsilon_r = 2.94$, thickness $h = 508$ μm, and $\tan\delta = 0.0012$. The metallisation thickness and conductivity are $t = 17.5$ μm and $\sigma = 5.8 \times 10^7$ S/m, respectively. The via diameter is $d = 1/64'$ (0.3969 mm) which is a standard drill size, and the via pitch is $p = 0.6$ mm, resulting in a d/p ratio of 0.6615. The substrate integrated waveguide width is 5.4 mm for a cut-off frequency of 17.2 GHz. For performance validation, a prototype of this design is fabricated and measured. Fig. 6 shows photographs of the fabricated system.

The tracking front end's performance depends on its sum and difference radiation patterns, gain and scattering parameters, all of

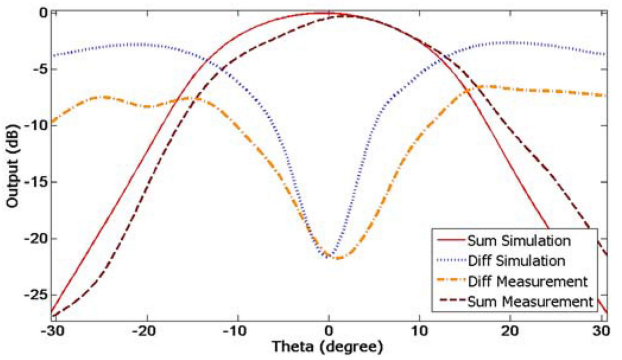

a

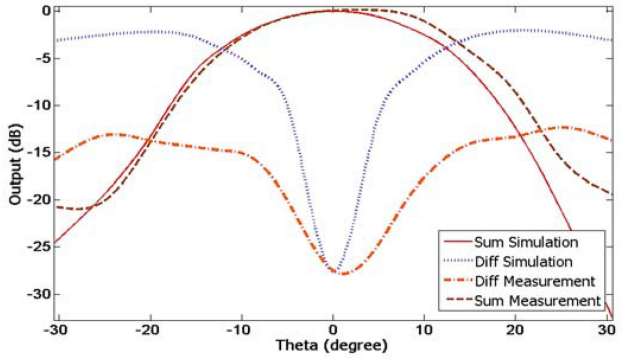

b

Fig. 7 *Measured and simulated sum and difference radiation patterns of the SIW tracking front end*
(a) 23.9 GHz, ***(b)*** 24.1 GHz

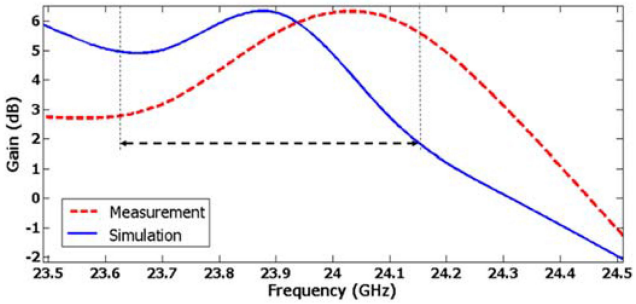

Fig. 8 *Gain comparison between measured and simulated results*

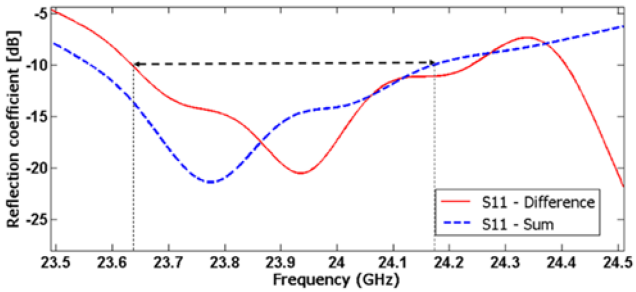

Fig. 9 *Measured reflection coefficient at sum and difference ports*

them are discussed in this section. The circuit is measured in a far field chamber using an Anritsu 37397C Vector Network Analyser.

Measurements and simulation results have a fairly good agreement; however, there are some discrepancies. This is due to the fact that the measured results are not obtained exactly under the same conditions as the simulation. In the simulations, a plane wave is used as a transmitter, which is able to move in spherical coordinates between $-180° \leq \theta \leq +180°$. In the measurements, a K-band standard gain horn antenna is used. Moreover, standard K-connectors are modelled in CST while during measurements, only larger end-launch connectors were available as shown in Fig. 6.

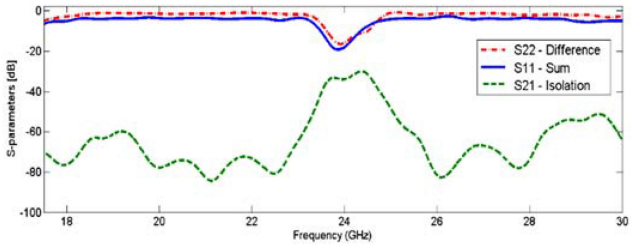

Fig. 10 *Measured system performance in sum and difference ports from 18 to 30 GHz*

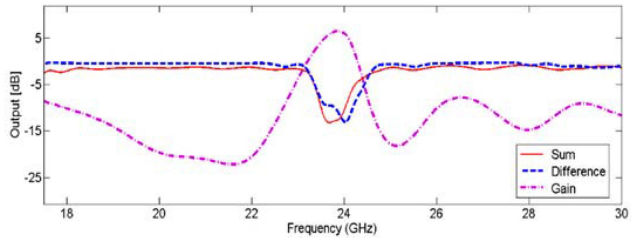

Fig. 11 *Simulated system performance in sum and difference ports as well as gain behaviour of the system from 18 to 30 GHz*

At two sample frequencies, Fig. 7 displays the signals at the sum and difference outputs as a function of incidence of the incoming wave. It is observed that this design has a 30° accurate target tracking from −15° to +15° over a 540 MHz bandwidth centred at 23.9 GHz. The measured field of view tracking is 32° and 42°, and the on-axis isolation is better than 22 and 27 dB at 23.9 and 24.1 GHz, respectively.

Fig. 8 shows the measured and simulated gains in the sum port versus frequency. The maximum gain is 6.2 dB with a slight frequency shift in measurements compared to simulations, which we attribute to slightly detuned resonators.

Measured return losses at the sum and difference ports are presented in Fig. 9. The return loss is better than 10 dB between 23.56 and 24.17 GHz at the sum port, and between 23.63 and 24.25 GHz at the difference port, which defines the operating bandwidth as 23.63–24.17 GHz. Therefore, the entire system provides an overall bandwidth of 540 MHz.

The inherent bandpass characteristic of the proposed system is depicted in Figs. 10 and 11. Fig. 10 shows the measured scattering parameters for sum and difference ports between 18 and 30 GHz. It also demonstrates the isolation between sum and difference ports which is better than 30 dB in the operating bandwidth and better than 60 dB at other frequencies between 18 and 30 GHz. Fig. 11 demonstrates the filtering response of the simulated results over a wider bandwidth. It shows that both gain and return loss only have the acceptable results in the defined operating band. These broadband measurements and simulations confirm that additional filtering components are not required owing to the frequency selective crossovers and bandpass power divider used in this design.

4 Conclusions

The design of a frequency-selective front-end system in single-layer SIW technology for tracking applications is presented. It operates at a centre frequency of 23.9 GHz with 540 MHz bandwidth and consists of two high gain Vivaldi antennas, two filtering SIW crossovers, and a sum-difference power combiner with a second-order filtering function. All individual components are designed and fine-optimised separately. The Vivaldi antenna is designed with a gain of 9.58 dB and good characteristics over a wide bandwidth from 19.2 to 28.6 GHz. The frequency-selective SIW crossover provides high isolation between its orthogonal arms which allows us to use it as a crossover transition between the Vivaldi antennas and the power combiner. The power combiner uses second-order filtering paths to provide in-phase and out-of-phase electric fields at sum and difference ports. The simulation and experimental results demonstrate the scanning ability of this

tracking front end over a 30-degree field of view. The proposed system has an on-axis isolation performance of better than 25, 22, and 27 dB in the difference port at 23.7, 23.9, and 24.1 GHz, respectively.

5 References

[1] Gezer, B.L.: 'Multi-beam digital antenna for radar, communications, and UAV tracking based on off-the-shelf wireless technologies'. Master Thesis, Dept. of Defence, Naval Postgraduate School, Monterey, CA, USA, 2006

[2] Sierra-Castaner, M., Sierra-Perez, M., Vera-Isasa, M., *et al.*: 'Low-cost monopulse radial line slot antenna', *IEEE Trans. Antennas Propag.*, 2003, **51**, (2), pp. 256–263

[3] Du, B., Yung, E.K.N., Yang, K.Z., *et al.*: 'Wideband linearly or circularly polarized monopulse tracking corrugated horn', *IEEE Trans. Antennas Propag.*, 2002, **50**, (2), pp. 192–197

[4] Tsai, Y.L., Hwang, R.B.: 'Time-division multiplexing monopulse antenna system for DVB-SH application', *IEEE Trans. Antennas Propag.*, 2015, **63**, (2), pp. 765–769

[5] Kumar, C., Kumar, V.S., Srinivasan, V.V.: 'Design aspects of a compact dual band feed using dielectric rod antennas with multiple element monopulse tracking', *IEEE Trans. Antennas Propag.*, 2013, **61**, (10), pp. 4926–4932

[6] Zhang, W., Cui, F., Wang, Q., *et al.*: 'Design of a waveguide slot array antenna for monopulse tracking application in millimeter wave'. Proc. 12th European Radar Conf., Paris, France, September 2015, pp. 469–472

[7] Yu, F., Xie, Y., Zhang, L.: 'Single patch antenna with monopulse patterns', *IEEE Microw. Wirel. Compon. Lett.*, 2016, **26**, (10), pp. 762–764

[8] Rezazadeh, N., Shafai, L.: 'Ultrawideband monopulse antenna with application as a reflector feed', *IET Microw. Antennas Propag.*, 2016, **10**, (4), pp. 393–400

[9] Cheng, Y.J., Hong, W., Wu, K.: 'Design of a monopulse antenna using a dual V-type linearly tapered slot antenna (DVLTSA)', *IEEE Trans. Antennas Propag.*, 2008, **56**, (9), pp. 2903–2909

[10] Liu, B., Hong, W., Yin, X., *et al.*: 'Substrate integrated waveguide (SIW) monopulse slot antenna array', *IEEE Trans. Antennas Propag.*, 2009, **57**, (1), pp. 275–279

[11] Yan, L., Hong, W., Wu, K.: 'Simulation and experiment on substrate integrated monopulse antenna'. IEEE AP-S Int. Symp. Digest, Washington, USA, July 2005, pp. 528–531

[12] Chen, H., Che, W., He, Q., *et al.*: 'Compact substrate integrated waveguide (SIW) monopulse network for Ku-band tracking system applications', *IEEE Trans. Microw. Theory Tech.*, 2014, **62**, (3), pp. 472–480

[13] Cheng, Y.J., Hong, W., Wu, K.: '94 GHz substrate integrated monopulse antenna array', *IEEE Trans. Antennas Propag.*, 2012, **60**, (1), pp. 121–129

[14] Connor, F.R.: 'New monopulse tracking radar', *IET Electron. Lett.*, 1983, **19**, (12), pp. 438–440

[15] Kordiboroujeni, Z., Bornemann, J.: 'Efficient design of substrate integrated waveguide power dividers for antenna feed systems'. Proc. 7th European Conf. Antennas Propagation, Gothenburg, Sweden, April 2013, pp. 352–356

[16] Bornemann, J., Rosenberg, U., Amari, S., *et al.*: 'Design of sum-difference power combiners with second-order filtering functions'. Proc. IEEE MTT-S Int. Conf. Numerical Electromagnetic Multiphysics Modeling Optimization (NEMO), Seville, Spain, May 2017, pp. 1–3

[17] Rosenberg, U., Salehi, M., Bornemann, J., *et al.*: 'A novel frequency-selective power combiner/divider in single-layer substrate integrated waveguide technology', *IEEE Microw. Wirel. Compon. Lett.*, 2013, **23**, (8), pp. 406–408

[18] Locke, L.S., Bornemann, J., Claude, S.: 'Substrate integrated waveguide-fed tapered slot antenna with smooth performance characteristics over an ultra-wide bandwidth', *Appl. Comput. Electromagn. Soc. (ACES) J.*, 2013, **28**, (5), pp. 454–462

[19] Kordiboroujeni, Z., Locke, L., Bornemann, J.: 'A diplexing antenna system in substrate integrated waveguide technology'. IEEE AP-S Int. Symp. Digest, Vancouver, Canada, July 2015, pp. 1042–1043

[20] Salem Hesari, S., Bornemann, J.: 'Substrate integrated waveguide crossover formed by orthogonal TE102 resonators'. Proc. 47th European Microwave Conf., Nuremberg, Germany, October 2017, pp. 1–4

[21] Deslandes, D.: 'Design equations for tapered microstrip-to-substrate integrated waveguide transitions'. IEEE MTT-S Int. Symp. Digest, Anaheim, USA, May 2010, pp. 704–707